

Experimental Determination of $\text{NH}_4\text{NO}_3\text{-KNO}_3$ Binary Phase Diagram

Wen-Ming Chien, Dhanesh Chandra, Abdel K. Helmy, Jennifer Franklin, and Claudia J. Rawn

(Submitted July 18, 2004; in revised form January 21, 2005)

The solid-state phase transitions in ammonium nitrate (AN)-potassium nitrate (KN) system, and the equilibrium AN-KN phase diagram have been determined by using differential scanning calorimetry and high-temperature in situ x-ray diffractometry. Sample preparation was performed in a special "dry room" with very low humidity. A single phase region (AN III) with no phase transitions to 373 K was observed in the composition range 5 to 20% KN; this is critical for use in air bag gas generators. The high-temperature KN phase (KN I) has a wide range of stability from 20 to 100 wt.% KN. There are one eutectic, two eutectoid, three peritectoid, and one congruent transformations in this phase diagram. Two new nonstoichiometric phases were found at lower temperatures in the mid-composition range between the AN and KN terminal solid solutions. Details of the phase equilibria are presented.

1. Introduction

Ammonium nitrate (NH_4NO_3 [AN]) is used as an oxidizer in propellants, explosives, and gas generators. It is well known that pure AN exhibits several solid-state phase transitions. In applications in the automotive industry, such as air bags, in which AN is used as an oxidizer, it is important to avoid these phase transitions because they cause volume changes with possible disintegration of the pellet or disk forms containing the oxidizer [1983Cad, 1983Chol and 1999Cha]. [1983Cad], [1975Hol], and [1992Dei] reported a method to stabilize the ANs by the addition of potassium nitrate (KNO_3 [KN]) to AN. [1932Jan] and [1949Jan] showed an AN-KN phase diagram for the entire AK-KN composition range; this is perhaps the first comprehensive study of this system. [1947Ber], [1955Mor], and [1963Coa] developed alternative AN-KN phase diagrams. [1981Cad] and [1983Cad] developed a phase diagram that was close to that of [1932Jan] in the range 0 to 30 wt.% KN. Comparison of these proposed phase diagrams show discrepancies among the phase transitions at lower temperatures, particularly so for the AN IV-AN III phases. In one of the phase diagrams, there is a simple line denoting a metastable phase change from AN IV to AN II. [1981Cad] and [1932Jan] have shown a two-phase AN IV + AN II region whereas the other four phase diagrams do not show this region. [1983Cad] and [1947Ber] showed two cubic phases, C_I and C_{II} , occurring at ~16 to 30 wt.% KN above 373K, but [1932Jan] reported only one cubic phase (C). In addition, there are uncertainties in the invariant equilibria temperatures and compositions. A more accurate determination of the phase diagram is important to

automotive, fertilizer, and propellant applications. Furthermore, modern instrumentation with environmentally controlled AN-KN sample preparation facilities minimize or eliminate effects of moisture on the solid-phase fields and pure compounds.

Pure AN has five different solid phases (i.e., AN V, AN IV, AN III, AN II, and AN I phases) and undergoes four different solid-state phase transitions before melting. The high-temperature AN I phase of pure AN is stable above 398 K and, before melting, is a *plastic phase* with a cubic structure having rotational disorder of the nitrate groups [1959Shi1]. The lattice parameter of the AN I phase cubic structure [1962Bro] with space group $Pm\bar{3}m$ is $a = 0.437$ nm and $Z = 1$. The tetragonal structure ($P4_21m$) of the AN II phase was reported to be stable between 357 and 398K [1959Shi2]. The lattice parameters of the AN II phase were determined by [1979Luc] as $a = 0.57193(1)$ nm and $c = 0.49326(1)$ nm ($Z = 2$). The crystal structure of the AN III phase of pure AN was determined as orthorhombic and stable between 305.3 and 357 K by x-ray studies [1947Goo]. [1980Luc] reported the crystal structure of AN III phase to be orthorhombic, space group $Pnma$, with $a = 0.77184(1)$ nm, $b = 0.58447(1)$ nm, and $c = 0.71624(1)$ nm ($Z = 4$) by a neutron diffraction study. A solid solution of the 5 wt.% KN was also determined as an AN III phase at room temperature, with a detailed structure study being performed by x-ray diffraction (XRD) [1976Hol] as well as by neutron diffraction [1980Cho, 1982Cho]. The next phase, AN IV, is stable between 255 and 305 K, and the structure was determined by [1932Wes], [1932Hen], and [1957Swa] as orthorhombic. More accurate structure information, particularly with regard to the structural role of the hydrogen atoms in the ammonium group, was determined by [1972Cho] with the neutron diffraction. [1979Luc] redetermined the orthorhombic structure ($Pmnn$) with the lattice parameters of $a = 0.57574(1)$ nm, $b = 6.5434(1)$ nm, and $c = 0.49298(1)$ nm ($Z = 2$). The structure of the AN V phase of AN was first reported by [1962Por] as tetragonal ($P4_2$) and was redetermined as orthorhombic with a space group of $Pccn$ by [1983Aht1]. The AN V phase is an or-

W.-M. Chien and D. Chandra, Metallurgical and Materials Engineering, MS 388, University of Nevada-Reno, Reno, NV 89557; A.K. Helmy, TRW Incorporated, Lockwood, NV 89434; J. Franklin, Sandia National Laboratory, Albuquerque, NM 87123; and C.J. Rawn, Oak Ridge National Laboratory, Oak Ridge, TN 37831. Contact e-mail: dchandra@unr.edu.

Section I: Basic and Applied Research

thorhombic structure and is stable below 257 K with [1983Aht1] finding lattice parameters of $a = 0.79804(1)$ nm, $b = 0.80027(1)$ nm, and $c = 0.98099(1)$ nm ($Z = 8$) at 233K, and [1983Cho2], finding lattice parameters of $a = 0.78850(2)$ nm, $b = 0.79202(2)$ nm, and $c = 0.97953(2)$ nm ($Z = 8$) at 78 K. The neutron diffraction study reported by [1983Aht2] showed that the AN V phase with orthorhombic structure was stable down to at least 5K.

Potassium nitrate undergoes one solid-state phase transition during heating with the KN I phase being stable above the transition temperature and the KN II phase below that temperature. The structure of the KN low-temperature KN II (α) phase has been studied by [1931Edw] and was redetermined by [1973Nim] who found an orthorhombic structure with the space group of $Pm\bar{c}n$ by using single-crystal neutron diffraction data. The unit cell of this orthorhombic structure is with $a = 0.54142$ nm, $b = 0.91659$ nm, and $c = 0.64309$ nm ($Z = 4$) at room temperature, and this was confirmed by [1975Hol] with single-crystal x-ray data. When KN is heated from room temperature, the KN II (α) \rightarrow KN I (β) phase transition occurs at ~ 401 K at atmospheric pressure. The high-temperature KN I phase structure was studied by [1947Tah], [1962Shi], and [1969Str], and the structure was determined by [1976Nim] as an hexagonal ($R\bar{3}m$) structure with $a = 0.5425(1)$ nm and $c = 0.9836(4)$ nm ($Z = 3$) at 424 K. [1939Bar] and [1969Str] reported that there is a metastable (ferroelectric) γ -phase of KN that appears during cooling of the KN I phase from high temperature to 397 K, and the γ -phase transformed to KN II phase at 373K. The crystal structure of the γ -phase was determined by [1976Nim] as hexagonal ($R\bar{3}m$) with $a = 0.5487(1)$ nm and $c = 0.9156(3)$ at 364K ($Z = 3$). [1969Str] reported the change in enthalpy associated with the $\beta \rightarrow \gamma$ phase transition as $3005.4 (\pm 8.4)$ J/mol at 396 K, and the corresponding transition entropy as $7.61 (\pm 0.21)$ J/(mol K). The enthalpy change of $\Delta H_{(\gamma \rightarrow \alpha)}$ was reported as $2336.6 (\pm 8.4)$ J/mol at 385 K.

The purpose of the present study was to determine the details of the solid-state phase transitions of AN-KN pseudobinary system. An experimental AN-KN phase diagram was obtained by using differential scanning calorimetry (DSC) and in situ high-temperature XRD.

2. Experimental

Ammonium nitrate is very sensitive to moisture, so the preparation of samples is a very important factor in the determination of the AN-KN equilibrium phase diagram. Several binary powder samples of different compositions were made using pure AN and KN powders. These samples were made in a special walk-in "dry room" with extremely low humidity at TRW (air bag propellant facility, Lockwood, NV). Thermodynamic analyses were performed using a computerized TA Instruments (New Castle, DE) differential scanning calorimeter for pure AN, pure KN, and the AN-KN samples. The enthalpies of phase transformations were measured along with the phase transformation onset and peak temperatures.

Crystal structure studies of the binary phases were per-

formed at the University of Nevada, Reno and at the Oak Ridge National Laboratories. Room-temperature powder diffraction work was performed using a Philips (Amsterdam, The Netherlands) Bragg-Brentano powder diffractometer in a nitrogen environment at University of Nevada, Reno. A plastic enclosure was installed around the room-temperature diffractometer. In addition, a desiccant (*Drierite*, Hammond Drierite Company, Xenia, OH) composed of anhydrous CaSO_4 (white) and 97wt.% CaSO_4 -3 wt.% COCl_2 (blue), was placed in the enclosure with constant nitrogen flow around the diffractometer, but a gas flow also was maintained within the sample holder. The humidity was monitored by a change in the color of 97wt.% CaSO_4 -3 wt.% CoCl_2 (blue). It is well known that the color changes from blue to purple if humidity is present. A cylinder of nitrogen was placed close to the chamber, and gas was released into the enclosure for approximately an hour before the experiment. The exiting gases were vented through a hood. Sample preparation (mixed with the internal standard Si or LaB_6) was done in the enclosure. After placing the sample in the diffractometer, an additional dry nitrogen gas flow was maintained directly to the sample holder housing such that there was minimal contact between water and the sample. X-ray data were recorded by the MDI DataScan program and were analyzed by the MDI Jade program (MDI, Materials Data, Inc., Livermore, CA).

The high-temperature XRD studies were performed by the high-temperature x-ray diffractometer at the High Temperature Material Laboratory, Oak Ridge National Laboratory. The samples were mixed with the internal standard (Si or LaB_6) and prepared in a glove bag with flowing nitrogen gas. The samples were placed on a heat strip (Rh, Pt) and were heated to the desired temperatures by the heat strip. After placing a sample in the diffractometer, the chamber was purged and evacuated three times with ultra high purity (UHP) He before an experimental run, and the He gas was kept flowing through the chamber during the experimental run. An experimental run for each sample was from room temperature to a temperature near the melting point of the solid, which had been determined from DSC results. The temperature range for an x-ray scan for each sample was preset by the Scintag software (Scintag, Inc., Sunnyvale, CA). The heating rate of the heat strip was $10^\circ\text{C}/\text{min}$. After an x-ray scan, there was a 5 min delay before the next scan was begun.

3. Results

The DSC pattern of pure AN with its different phases is shown in Fig. 1(a). The first endotherm is observed at 270.43 K with a very low enthalpy of transition of 120.07 J/mol, and this is attributed to the V \rightarrow IV phase transition. Another endotherm observed at 325.73 K is attributed to the IV \rightarrow III phase transition. The next endotherm observed at 361.72 K is that of the III \rightarrow II phase transition. The II \rightarrow I phase transition occurs at 399.58 K. The melting point is at 442.28 K, and AN becomes gas at 526.53 K. The XRD results for pure AN in the temperature range from 293 to 423 K are shown in Fig. 1(b). The different phases are

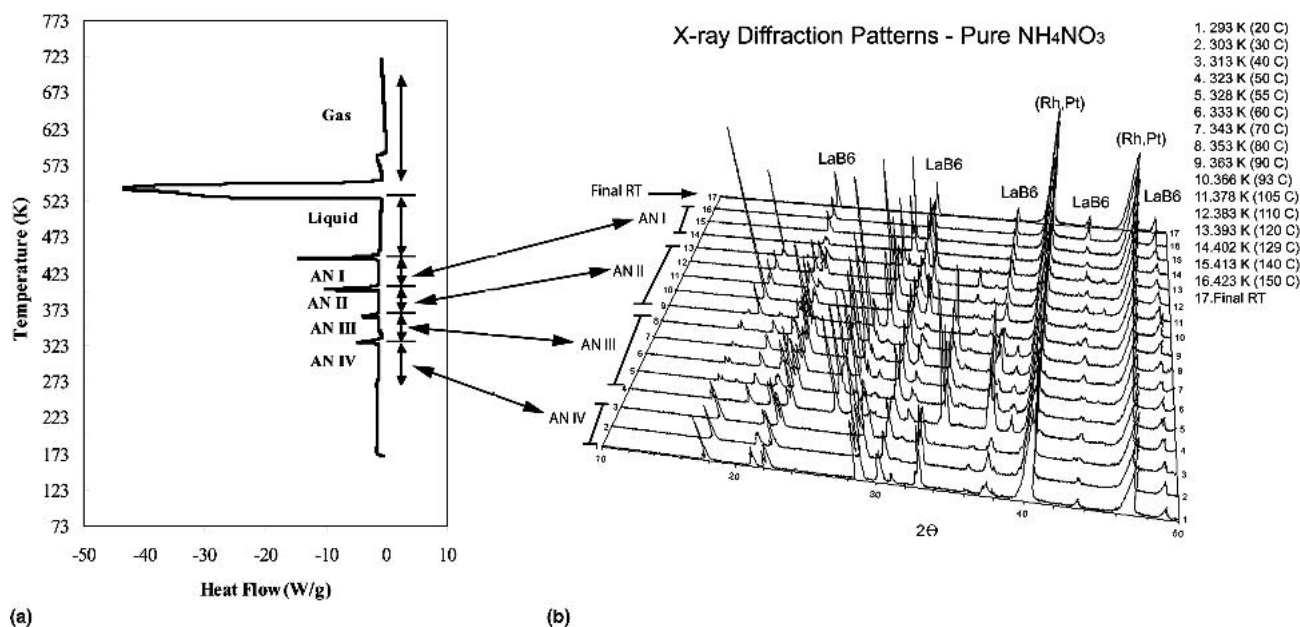


Fig. 1 (a) DSC results and (b) XRD patterns, which together show the phase transitions for the different phases of pure AN. The x-ray peaks, marked as LaB_6 , are the internal standard, and (Rh,Pt) are the heating strip.

indicated on the left-hand side with the arrows pointed to the corresponding phases in the DSC results. The XRD patterns taken at 293 to 313 K (marked as No. 1-3) show the AN IV phase with the orthorhombic ($Pmnm$) structure, and these results match the DSC data in the AN IV phase range (270.43-325.73 K). The AN III phase (orthorhombic structure with $Pbnm$ space group) shows the XRD patterns in the temperature range of 323 to 353 K (No. 4-8) and in the DSC data in the temperature range 325.73 to 361.72 K. The No. 9 to 13 XRD patterns (363-393 K) show the AN II phase (tetragonal with $P4bm$) and match the DSC results in the range 361.72 to 399.58 K. The DSC results show the AN I phase (cubic) in the temperature range of 399.58 to 422.28 K and match the XRD patterns (402-423 K) in No. 14 to 16. The AN V, liquid, and gas phases are not shown in XRD patterns, because these phases are out of the accessible XRD temperature range (i.e., from room temperature to 423 K). It should be noted that neither intensities nor positions of the peaks for the internal standard (LaB_6) and heating strip (Rh, Pt) change significantly in this temperature range. The x-ray pattern marked as "Final RT" in Fig. 1(b) is the x-ray pattern taken at the sample, which is cooled from 423 K down to room temperature, and comparison of this pattern with the x-ray pattern taken at room temperature before heating indicates a non-equilibrium condition.

The DSC result, XRD patterns (293-428 K), and the partial AN-KN phase diagram (up to 5 wt.% KN composition) of the 97wt.%AN-3wt.%KN solid solution with the phase transitions are shown in Fig. 2. The 3 mol.% KN room temperature XRD pattern shows both AN IV + AN III phases, and this persists to 318 K. The AN IV + AN III two-phase region is found in 2 to 4 wt.% KN compositions at room temperature, as shown in the AN-KN phase diagram. The DSC results indicates the AN IV + AN III \rightarrow AN III boundary to be 314.82 K. The AN III phase was ob-

served at the 328 and 343 K by XRD. The AN III \rightarrow AN II phase transition occurs at 374.26 K, and the AN II phase appears in the 383 K XRD pattern. As the temperature increases, the AN II \rightarrow AN I phase transition occurs at 399.31 K, and the 413 K XRD pattern is that of the AN I phase. The DSC results also show that the AN I \rightarrow liquid, liquid \rightarrow L + G, and L + G \rightarrow gas phase transitions occurs at 437.02, 532.58, and 545.75 K, respectively. The detail phase transition temperatures and enthalpies for different AN-KN compositions are showing in Table 1.

As the composition increases to 5 wt.% KN, the DSC scan from room temperature upward shows no phase transition until 377.87 K in Fig. 3(b). This result is important for air bag applications. The XRD patterns taken from 293 to 373 K are identified as a single AN III phase, which confirms the DSC results. The XRD patterns taken at 293 and 373 K in Fig. 3(a) can be indexed as the AN III phase. In contrast to the XRD patterns of the pure AN and 3 wt.% KN samples, there is no AN IV phase in the 5 wt.% KN XRD patterns. At higher temperatures, 5 wt.% KN XRD patterns show the AN II and AN I phases, which is similar to the results from the 3 wt.% KN solid solution. Patterns 3 and 4 in Fig. 3(a) show the XRD patterns, which can be indexed as the AN II phase at 388 K and the AN I phase at 408 K. The AN III \rightarrow AN II and AN II \rightarrow AN I phase transitions occur at 399.15 and 435.49 K, respectively, in 5 wt.% KN sample.

Figure 4 shows the different phases at various compositions in the AN-KN system. Representative diffraction patterns for selected compositions are shown in the lower part of the figure and are for a temperature between 303 and 318 K. The phase boundaries were determined from the different Bragg peaks appearing at different diffraction patterns compositions. At point 1 (pure AN) in Fig. 4, the XRD pattern is identified as the AN IV phase at 313 K, and point 2 (97wt.%AN-3wt.% KN) as the AN IV + AN III mixed

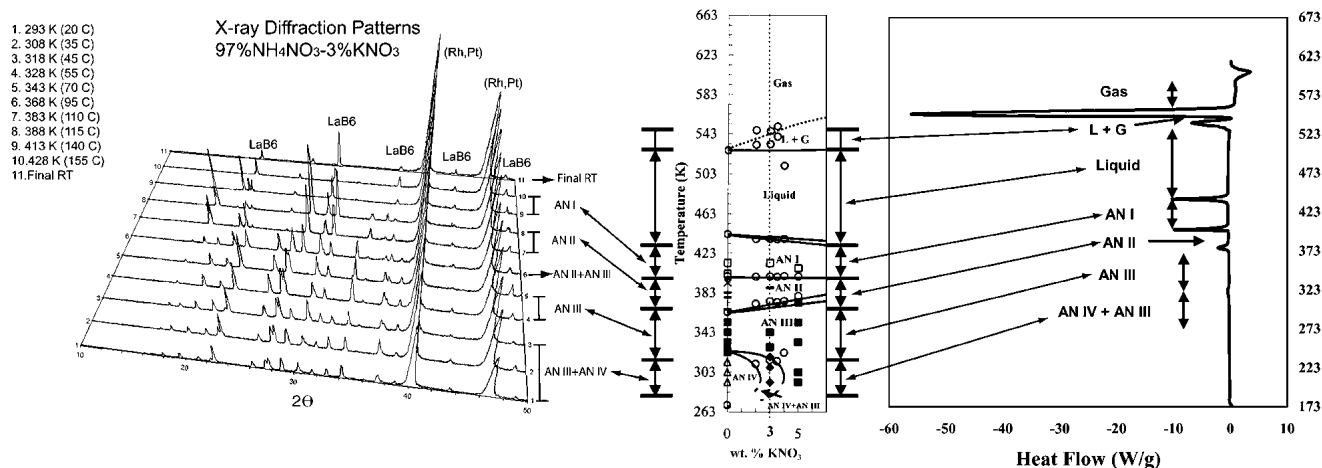


Fig. 2 The DSC result, XRD patterns (293-428 K), and the partial AN-KN phase diagram (up to 5 wt.% KN composition) of the 97wt.% AN-3wt.% KN solid solution with the phase transitions for different phases.

Table 1 The transition temperatures (T_t) and enthalpies (ΔH) of the phase transitions for the $\text{NA}_4\text{NO}_3\text{-KNO}_3$ solid solutions

Composition (wt.% KNO_3)	(AN IV + AN III) \rightarrow AN III		AN III \rightarrow AN II		AN II \rightarrow AN I		AN I \rightarrow L	
	T_t , K	ΔH , kJ/mol	T_t , K	ΔH , kJ/mol	T_t , K	ΔH , kJ/mol	T_t , K	ΔH , kJ/mol
2	311.12	0.273	371.65	1.131	399.12	3.755	437.24	4.944
3	314.82	0.252	374.26	1.394	399.31	3.931	437.50	5.148
3.5	314.02	0.190	373.37	1.412	399.16	4.228	437.02	5.538
4	322.42	0.060	374.87	1.525	399.79	4.258	437.19	5.589
5	377.87	1.404	399.15	3.896	435.49	5.104
6	381.46	1.520	399.36	4.071	433.91	5.344

Composition (wt.% KNO_3)	ANZ + KN II \rightarrow KN I		KN II \rightarrow KN I		KN I \rightarrow L	
	T_t , K	ΔH , kJ/mol	T_t , K	ΔH , kJ/mol	T_t , K	ΔH , kJ/mol
92	394.03	5.494	591.45	9.539
95	396.61	6.784	596.91	10.516
98	398.89	6.418	602.62	10.552
100	402.79	6.437	605.07	11.172

phases at 318 K. The low-temperature AN III phase is stable from 5 to 20 wt.% KN (point 3 to point 4) shown in AN-KN phase diagram in the top portion of Fig. 4. The XRD pattern of point 5 (30 wt.% KN at 313 K) shows the AN III phase along with Bragg peaks marked “**” from an ANK phase. The x-ray pattern of point 6 (50 wt.% KN at 313 K) is similar to that of point 5, but with the higher intensity of the extra Bragg peaks. This AN III + ANK two-phase region persists to 353 K. In the composition range of 80 to 92 wt.% KN (point 7 to point 8), the XRD patterns show the KN II and ANZ mixed phases, and this two-phase region persists to 393 K. The low-temperature KN II single phase with an orthorhombic ($Pnma$) structure is found in the XRD pattern at point 9 and point 10 (95 to 100 wt.% KN) and is stable from room temperature to 393 K. A partial phase diagram of 75 to 100 wt.% KN in the 353 to 493 K temperature range is shown together with x-ray patterns in Fig. 5(a) and (b). At 373 K, the XRD pattern at point 1 (98 wt.% KN) shows only

the KN II phase with no indication of the ANZ phases while point 2 (80 wt.% KN) shows both KN II and ANZ phases. The XRD patterns of both point 3 (98 wt.% KN at 453K) point 4 (80 wt.% KN at 463 K) show only the high-temperature KN I phase with trigonal ($R3m$) symmetry.

The proposed AN-KN phase diagram is shown in Fig. 6 and is based upon both DSC and XRD results. In low-temperature phase regions, a single (AN III) phase region without any phase transitions between 293 and 373 K was observed for compositions between 5 and 20 wt.% KN in AN, which is critical for air bag gas generator applications. Other low-temperature phase regions include the AN III + ANK, ANK + ANZ, and ANZ + KN II two-phase regions, and the ANK, ANZ, and KN II single-phase regions. The higher-temperature KNO_3 (KN I) phase has a wide stability range from 20 to 100 wt.% KN solid solutions. The boundaries of the (gas + liquid), ANK, and ANZ phase regions in Fig. 6 are marked with dotted lines because these phase

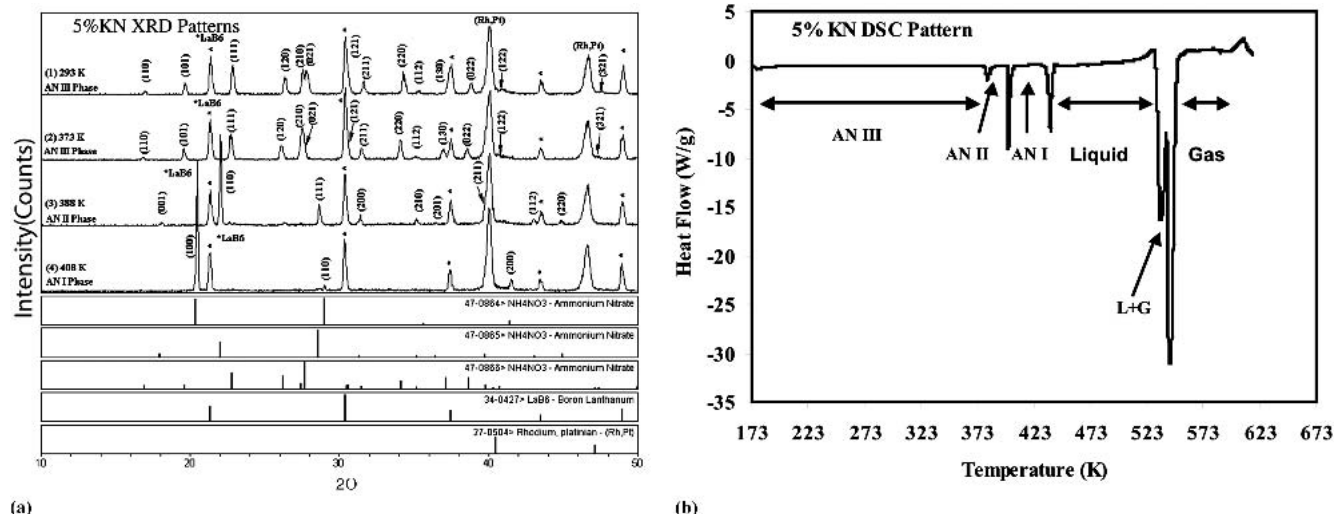


Fig. 3 (a) The 5 wt.% KN XRD patterns show the AN III phase at pattern No. 1 (293K) and pattern No. 2 (373K), the AN II phase at pattern No. 3 (388K), and the AN I phase at pattern No. 4 (408K). (b) The 5 wt.% KN DSC scan shows the different phases, and there is no phase transition up to 377.87K.

regions are not well determined. There are two new proposed non-stoichiometric solid phases, ANK and ANZ, that have been proposed for the AN-KN phase diagram. The ANK region of homogeneity is in the vicinity of 53 to ~56 wt.% KN and is stable up to ~429 K, while the range of homogeneity of ANZ is ~72 to ~74 wt.% KN with stability to ~425 K. No detailed structural information for either ANK and ANZ is available. The AN II + AN I two-phase region is estimated to be very narrow because the AN II to AN I transition temperature is only slightly below the temperature of the peritectoidal decomposition of the AN II terminal solid solution. In the proposed AN-KN phase diagram there are seven invariant equilibria: one eutectic, $L \rightarrow AN I + KN I$ at 16 wt.% KN and 429 K; two eutectoids, $KN I \rightarrow AN III + ANK$ at 39 wt.% KN and 373 K, and $KN I \rightarrow ANZ + KN II$ at 88 wt.% KN and 393 K; three peritectoids, $AN II + KN I \rightarrow AN III$ at 14 wt.% KN and 390 K, $ANZ + KN I \rightarrow ANK$ at 55 wt.% KN and 380 K, and $AN I + KN I \rightarrow AN II$ at 8 wt.% KN and 400 K; and one congruent transition, $KN I \rightarrow ANZ$ at 72 wt.% KN and 415 K. Compositions and temperature for these invariants are given in Table 2.

4. Discussion

In pure dry AN, the present investigation found the solid-state phase $AN IV \rightarrow AN III$ transition at 325.7 K; in the presence of moisture the transition temperature was reported as 305.3K by both [1947Goo] and [1972Cho]. For very dry AN, a direct $AN IV \rightarrow AN II$ phase transition (instead of $AN IV \rightarrow AN III$ and $AN III \rightarrow AN II$) at 328 K was suggested by [1962Bro] and [1979Luc]. In this study, under a moisture-free environment, the DSC results show that there is a phase transition observed at 325.73 K, which is ~20 K higher than the transition temperature of $AN IV \rightarrow AN III$ reported by [1947Goo] and [1972 Cho], is close to the transition temperature of $AN IV \rightarrow AN II$ reported by

[1962Bro] and [1979Luc]. However, our SRD data showed that the AN IV phase transitions to AN III rather than AN II with AN III being stable between 328 and 363 K (Fig. 1). The present results indicate that the phase transition at 325.73 K is the $AN IV \rightarrow AN III$ phase transition.

Many investigators [1975Hol, 1982Cho, 1983Cad, 1992Dei] have used a variety of different inorganic compounds to obviate phase transitions in AN near room temperature. These include hexamminenickel nitrate, $CsNO_3$, and KN. Indeed, [1983Cad] suggested that KN would stabilize the AN III phase. This is in agreement with the present results, which quantify the necessary amount of KN as being in the composition range 5 to 20 wt.% KN.

[1981Cad] and [1983Cad] reported an AN-KN phase diagram for the AN-rich end up to 30 wt.% KN. Comparison of the AN-KN phase diagram of [1981Cad] and [1983Cad] with the presently proposed diagram shows reasonable agreement in the 0 to 30 wt.% KN region. The significant difference is showing in $AN IV \leftrightarrow AN III$ phase boundary. This AN IV phase transformed directly to the AN III phase without passing through an $AN IV + AN III$ two-phase region. The present XRD results show definitively that there is $AN IV + AN III$ two-phase in 3 wt.% KN composition at room temperature and higher; the existence of a two-phase region is in conformity with the phase rule. So, we proposed that the $AN IV + AN III$ two-phase region is located through the region of 2 to 4 wt.% KN near room temperature. [1981Cad] and [1983Cad] also reported a "metastable" phase transition line of $AN IV \leftrightarrow AN II$ that occurs at 325 K in pure AN sloping down to 315 K at 10 wt.% in KN; this line was not observed in the present study. The result may represent an $AN IV + AN III$, $AN IV + AN III/AN III$, $AN III$ boundary separating $AN IV + AN III$ from AN III, as shown in our phase diagram rather than the metastable phase transition line of $AN IV \leftrightarrow AN II$. It is interesting to note that both the data of [1981Cad] and [1983Cad], Cady's and our data show a stable KN phase

Section I: Basic and Applied Research

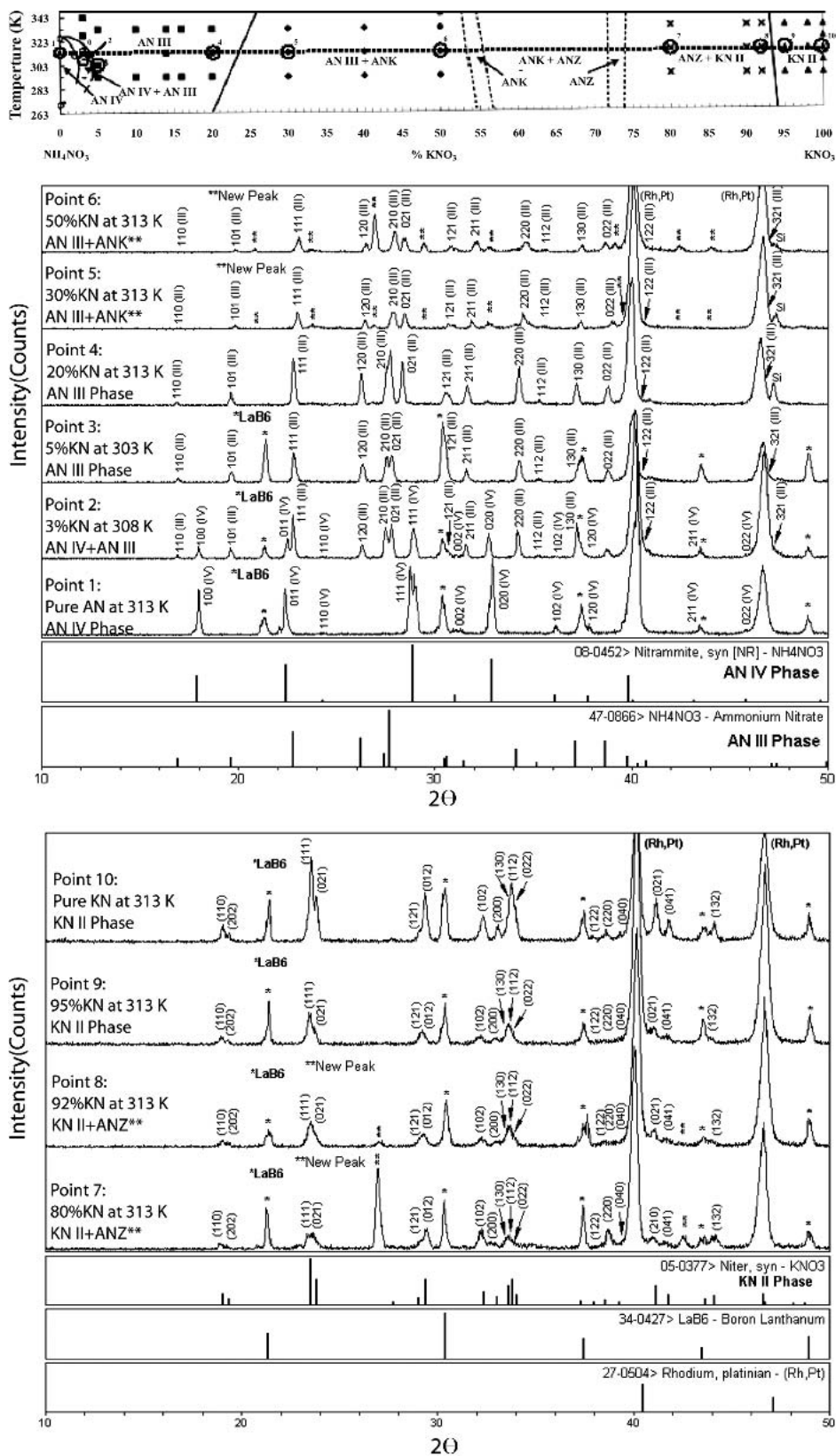


Fig. 4 The low-temperature phases in the different compositions of AN-KN solid solutions as well as the XRD patterns at the temperature range of 303 to 318K. The single-phase region appears at point 1 (AN IV), point 3 (AN III), point 4 (AN III), point 9 (KN II), and point 10 (KN II). The two-phase regions appear at point 2 (AN IV + AN III), point 5 (AN III + ANK), point 6 (AN III + ANK), point 7 (ANZ + KN II), and point 8 (ANZ + KN II).

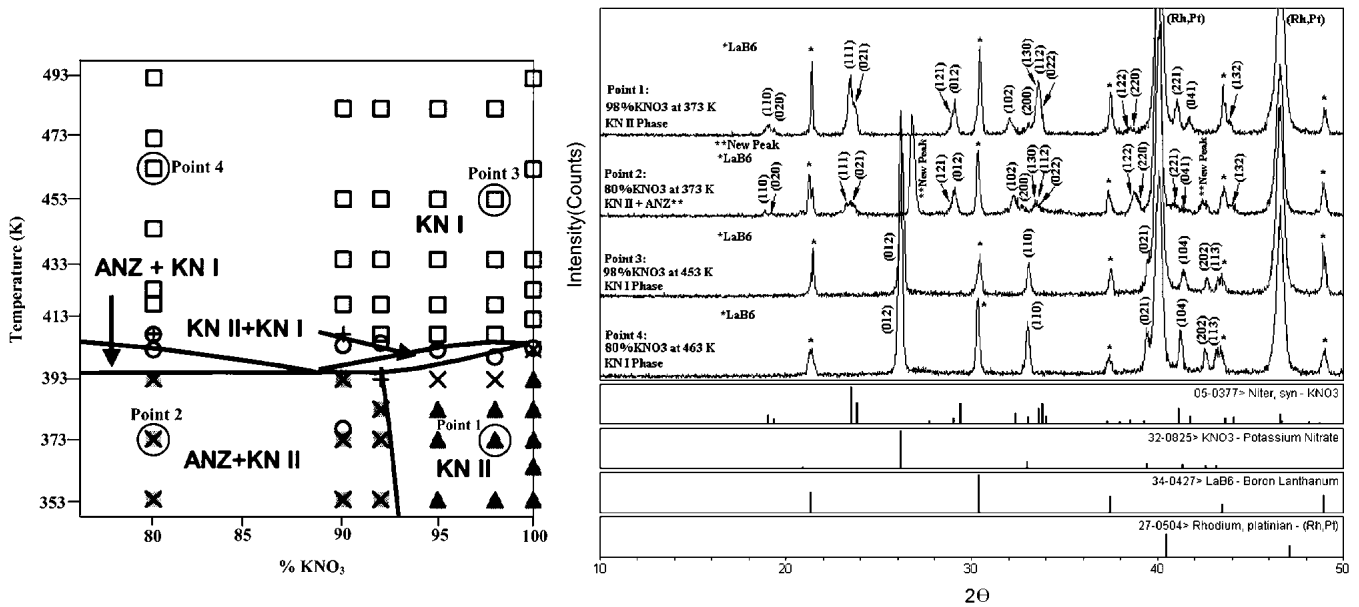


Fig. 5 (a) The partial phase diagram of 75 to 100 wt.% KN composition range and 353 to 493K temperature range, and (b) the x-ray patterns with indexing of 80 and 98 wt.% KN solids, which show the KN II, ANZ + KN II, and KN I phase regions

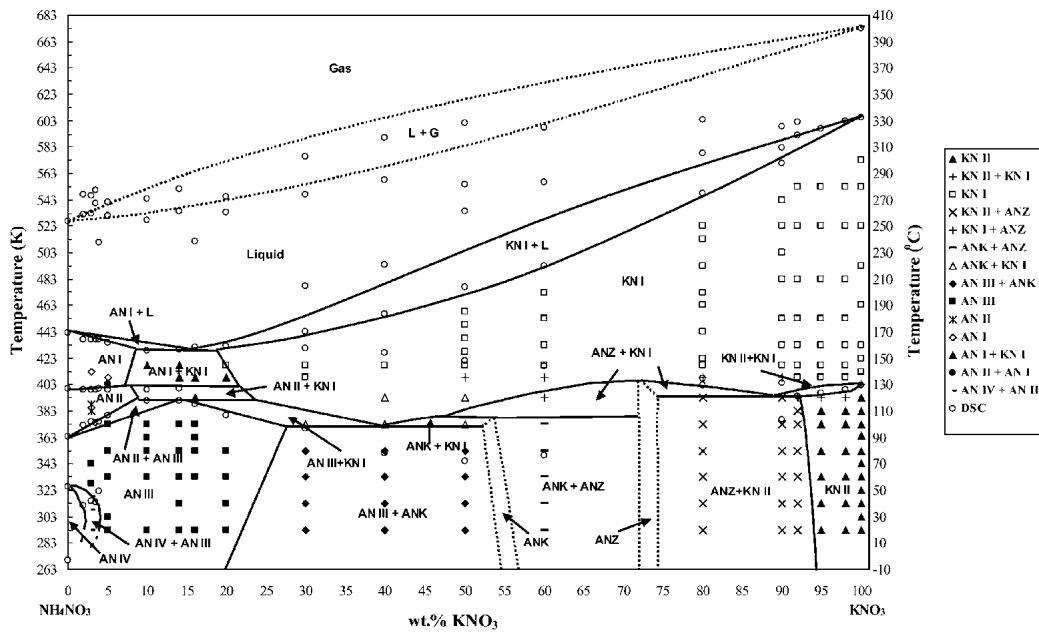


Fig. 6 The proposed AN-KN phase diagram

protruding to about 20 wt.% KN. The present results show no indication of C_I and C_{II} phases as reported by [1981Cad] and [1983Cad]. Other discrepancies involve the two-phase fields labeled as $AN_{II} + C_{II}$ and $AN_I + C_{II}$ phase regions in phase diagram of [1981Cad] and [1983Cad]; the present diagram interprets these as $AN_{II} + KN_{I}$ and $AN_{I} + KN_{I}$ two-phase regions, respectively.

The AN-KN phase diagram reported by [1932Jan] and [1949Jan] showed a eutectic ($L \rightarrow AN_I + KN_{I}$) at 430K that is matched in the results of both [1981Cad] and [1983Cad],

and the present study. A peritectoid, $AN_{II} + KN_{I} \rightarrow AN_{III}$, at 390 K was found in this study, but it is missing in the phase diagram of [1981Cad] and [1983Cad]. A similar peritectoid, $AN_{II} + C \rightarrow AN_{III}$, was also found in the phase diagram of [1932Jan] and [1949Jan] at 383 K. The K_1 and K_2 phase regions in the phase diagram of [1932Jan] and [1949Jan] are matched in the present phase diagram by KN_{I} and KN_{II} phases, respectively. Only one single K_3 phase is shown near mid-range composition of the phase diagram of [1932Jan] and [1949Jan], but it is now proposed to in-

Section I: Basic and Applied Research

Table 2 The invariant equilibria in $\text{NA}_4\text{NO}_3\text{-KNO}_3$ phase diagram

Invariant equilibria	Composition (wt.% KNO_3)			Temperature, K ($^{\circ}\text{C}$)
	AN I	L	KN I	
Eutectic: L \rightarrow AN I + KN I	AN I 10	L 16	KN I 20	429 (155.85)
Eutectoid 1: KN I \rightarrow AN III + ANK	AN III 27	ANK 39	KN I 53	373 (99.85)
Eutectoid 2: KN I \rightarrow ANZ + KN II	ANZ 74	KN I 88	KN II 93	393 (119.85)
Peritectoid 1: AN II + KN I \rightarrow AN III	AN II 10	AN III 14	KN I 24	390 (116.85)
Peritectoid 2: ANZ + KN I \rightarrow ANK	KN I 47	ANK 55	ANZ 72	380 (106.85)
Peritectoid 3: AN I + KN I \rightarrow AN II	AN I 7	AN II 8	KN I 22	400 (126.85)
Congruent: KN I \rightarrow ANZ	...	ANZ 72	...	415 (141.85)

clude two single-phases, ANK and ANZ, in the present phase diagram. The C phase region showed in the phase diagram of [1932Jan] and [1949Jan] is similar to the C_I and C_{II} in that of [1981Cad] and [1983Cad], and it is the KN I phase region in this study. In the low-temperature region, [1932Jan] and [1949Jan] showed a wide range (up to 30 wt.% KN) of AN IV + AN III two-phase region compared to the present narrow two-phase region. Other AN-KN phase diagrams reported by [1947Ber], [1955Mor] by differential thermal analysis curves, and [1963Coa] by XRD results are in poor agreement with present results. Two new nonstoichiometric phases, ANK and ANZ, are now proposed on the basis of the diffraction data, but these data are as yet inadequate for structure determination.

Establishment of the range of stability of the AN III phase was one important reason for undertaking the present investigation, and results indicate that the phase is stable up to 362 K or higher in the composition range 0 to ~28 wt.% HNO_3 . At 325.7 K, AN III transforms to AN IV in pure AN. As the temperature is lowered below this transition temperature, a two-phase field extends from the AN transition with the (AN IV + AN III)/AN III boundary reaching a maximum HNO_3 content of between 4 and 5 wt.% a few degrees below 325 K. As the temperature is further reduced, the boundary moves back toward lower HNO_3 contents (data in AN IV + AN III \rightarrow AN III columns of Table 1). However, no measurements were made at room temperatures below 293 K. Therefore, the extrapolation of the AN IV/(AN IV + AN III) and the (AN IV + AN III)/AN III boundaries below 293 K are uncertain and are dashed for only a short temperature range below that temperature in Fig. 2, 4, and 6. Certainly, these two boundaries cannot converge at the AN V \rightarrow AN IV transition of pure AN because this would imply the coexistence of AN V, AN IV, and AN III at the same temperature and composition in violation of the phase rule. With this terminus precluded, the two boundaries may be extrapolated to participate in (a) a peritectoidal decomposition of an AN V-terminal solid

solution, AN V \rightarrow AN IV + AN III at a temperature above the pure AN transition, or (b) a eutectoidal dissociation of AN IV as AN IV \rightarrow AN V + AN III below the pure AN transition. In either case, the phase richest in HNO_3 would be AN III with composition <2 to 3 wt.% HNO_3 . The implication is that the AN III single-phase field remains quite wide at temperatures significantly below the experimental temperature range of measurement, so the phase should remain stable at still lower temperatures. This is relevant if the oxidizer is to be used in far northern latitudes.

5. Conclusions

The solid-state phase transitions in AN-KN solid solutions and the equilibrium AN-KN phase diagram were determined, and we have resolved issues related to phase stabilities in AN-rich regions. The AN III phase region is stable between 5 to 20 wt.% KN, up to ~373 K in temperature; this is critical for the air bag gas generators. The high-temperature KN I phase is stable over a wide composition range of 20 to 100 wt.% KN. Two newly proposed single phases, ANK and ANZ, are located in the mid-range of the phase diagram. The AN-KN phase diagram contains one eutectic, two eutectoid, three peritectoid, and one congruent transition.

Acknowledgments

The authors are very grateful for the financial support of this project to TRW Inc. (Lockwood, NV), and to its management and staff. We also thank Dr. Abdel Helmy of TRW for his continuous input in support of this research. The authors would also like to acknowledge Dr. Claudia Rawn of the Oak Ridge National Laboratory for help and for the use of a high-temperature x-ray diffractometer.

References

- 1931Edw: D.A. Edwards, A Determination of the Complete Crystal Structure of Potassium Nitrate, *Z. Kristallogr.*, Vol 80, 1931, p 154-163
- 1932Hen: S.B. Hendricks, E. Posnjak, and F.C. Kracek, Molecular Rotation in the Solid State. The Variation of the Crystal Structure of Ammonium Nitrate with Temperature, *J. Am. Chem. Soc.*, Vol 54, 1932, p 2766-2786
- 1932Jan: Von E. Jänaecke, H. Hamacher, and E. Rahlds: Über das System $\text{KNO}_3\text{-NH}_4\text{NO}_3\text{-H}_2\text{O}$, *Z. Anorg. Allg. Chem.*, Vol 206, 1932, p 357-368 (in German)
- 1932Wes: C.D. West, The Crystal Structure of Rhombic Ammonium Nitrate, *J. Am. Chem. Soc.*, Vol 54, 1932, p 2256-2260
- 1939Bar: T.F.W. Barth, Crystal Structure of the Pressure Modification of Salt-Peter, *Z. Phys. B: Condens. Mater.*, Vol 43, 1939, p 448-450
- 1947Ber: A.G. Bergman, V.P. Radishchev, I.N. Nikonova, V.N. Sveshnikova, E.B. Shternina, and M.A. Yatsuk, External Components of the Fusion Diagram of the Quaternary Reciprocal System NH_4 , KlCl , NO_3 , H_2PO_4 , *Izvest. Sektora Fiz.-Khim. Anal., Inst. Obshch. Neorg. Khim., Akad. Nauk S.S.S.R.*, Vol 15, 1947, 157-199
- 1947Goo: T.H. Goodwin and J. Whetstone, The Crystal Structure of Ammonium Nitrate III, and Atomic Scattering Factors in Ionic Crystals, *J. Chem. Soc. Abs.*, November 1947, p 1455-1461
- 1947Tah: P.E. Tahvonen, X-ray Investigation of Molecular Rota-

- tion in Potassium Nitrate Crystals, *Ann. Acad. Sci. Fennicae*, Vol A (I. Math.-Phys. No. 44), 1947, p 20
- 1949Jan:** Von E. Jänecke, Über das Ternares System der Nitrate von Kalium, Natrium and Ammonium (K, Na, NH_4)NO₃, *Z. Anorg. Allg. Chem.*, Vol 259, 1949, p 92-106 (in German)
- 1955Mor:** J. Morand, Ammonium Nitrate and Its Solid Solutions, *Ann. Chim. (Paris)*, Vol 10, 1955, p 1018-1060 (in French)
- 1957Swa:** H.E. Swanson, N.T. Gilfrich, and M.I. Cook, Standard X-ray Diffraction Powder Patterns, *Natl. Bur. Std. Circular*, Vol 539, 1957, p 70
- 1959Shi1:** Y. Shinnaka, X-ray Study of Molecular Rotation in Cubic Ammonium Nitrate, *J. Phys. Soc. Jpn.*, Vol 14, 1959, p 1073-1083
- 1959Shi2:** Y. Shinnaka, X-ray Study on Molecular Rotation in Tetragonal Ammonium Nitrate, *J. Phys. Soc. Jpn.*, Vol 14, 1959, p 1707-1716
- 1962Bro:** R.N. Brown and A.C. McLaren, The Mechanism of the Thermal Transformations. *Proc. Royal Society*, Vol 266, 1962, p 329-343
- 1962Por:** J.L.A. Portoles, F. Arrese, and M.L. Canut, The Crystal Structure of the Low-Temperature Phase of NH₄NO₃(V) at -150°, *Z. Kristallogr.*, Vol 117, 1962, p 92-107
- 1962Shi:** Y. Shinnaka, X-ray Study on Disordered Structure Above the Ferroelectric Curie Point in Potassium Nitrate, *J. Phys. Soc. Jpn.*, Vol 17, 1962, p 820-828
- 1963Coa:** R.V. Coates and G.D. Woodward, X-ray Powder Diffraction Data for Solid Solutions and Double Salts Occurring in Granular Compound Fertilizers, *J. Sci. Food Agric.*, Vol 14, 1963, p 398-404
- 1969Str:** K.O. Stromme, On the Structure of Potassium Nitrate in the High Temperature Phase I and III, *Acta Chem. Scand.*, Vol 23 (No. 5), 1969, p 1625-1636
- 1972Cho:** C.S. Choi, J.E. Mapes, and E. Prince, The Structure of Ammonium Nitrate (IV), *Acta Crystallogr., Sect. B*, Vol 28, 1972, p 1357-1361
- 1973Nim:** J.K. Nimmo and B.W. Lucas, Neutron Diffraction Determination of The Crystal Structure of α -Phase Potassium Nitrate at 25 °C and 100 °C, *J. Phys. C: Solid State Phys.*, Vol 6 (No. 2), 1973, p 201-211
- 1975Hol:** J.R. Holden and C.W. Dickinson, Crystal Structure of Three Solid Solution of Ammonium Nitrate and Potassium Nitrate, *J. Phys. Chem.*, Vol 79 (No. 3), 1975, p 249-256
- 1976Nim:** J.K. Nimmo and B.W. Lucas, The Crystal Structure of γ - and β -KNO₃ and the $\alpha \leftarrow \gamma \leftarrow \beta$ Phase Transformations, *Acta Crystallogr. Sect. B*, Vol B32 (No. 7), 1976, p 1968-1971
- 1979Luc:** B.W. Lucas, M. Ahtee, and A.W. Hewat, The Crystal Structure of Phase II Ammonium Nitrate, *Acta Crystallogr., Sect. B*, Vol B35, (No. 5), 1979, p 1038-1041
- 1980Cho:** C.S. Choi, H.J. Prask, and E. Prince, Phase Transitions in Ammonium Nitrate, *J. Appl. Crystallogr.*, Vol 13, (No. 5), 1980, p 403-409
- 1980Luc:** B.W. Lucas, M. Ahtee, and A.W. Hewat, The Structure of Phase III Ammonium Nitrate, *Acta Crystallogr., Sect. B*, Vol B36 (No. 9), 1980, p 2005-2008
- 1981Cad:** H.H. Cady, The Ammonium Nitrate-Potassium Nitrate System, *Propellants and explosives*, Vol 6, 1981, p 329-343
- 1982Cho:** C.S. Choi and H.J. Prask, Single-Crystal Neutron Diffraction Study of Ammonium Nitrate Phase III, *Acta Crystallogr., Sect. B*, Vol B38 (No. 9), 1982, p 2324-2328
- 1983Aht1:** M. Ahtee, K.J. Smolander, B.W. Lucas, and A.W. Hewat, The Structure of the Low-Temperature Phase V of Ammonium Nitrate, NH₄NO₃, *Acta Crystallogr., Sect. C*, Vol C39 (No. 6), 1983, p 651-655
- 1983Aht2:** M. Ahtee, K.J. Smolander, B.W. Lucas, and A.W. Hewat, Low-Temperature Behavior of Ammonium Nitrate by Neutron Diffraction, *Acta Crystallogr., Sect. B*, Vol B39 (No. 6), 1983, p 685-687
- 1983Cad:** H.H. Cady, Phase Stabilization of Ammonium Nitrate, CPIA Publication No. 377, Johns Hopkins University, Applied Physics Laboratory, Baltimore, MD, 1983, p 9-14
- 1983Cho1:** C.S. Choi and H.J. Prask, Phase Stabilization of Ammonium Nitrate, CPIA Publication No. 377, Johns Hopkins University, Applied Physics Laboratory, Baltimore, MD, 1983, p 87-96
- 1983Cho2:** C.S. Choi and H.J. Prask, The Structure of Ammonium Nitrate-d4 Phase V by Neutron Powder Diffraction, *Acta Crystallogr., Sect. B*, Vol B39 (No. 4), 1983, p 414-420
- 1992Dei:** A. Deimling, W. Engel, and N. Eisenreich, Phase Transitions of Ammonium Nitrate Doped with Alkali Nitrates Studied with Fast X-ray Diffraction, *J. Therm. Anal.*, Vol. 38, 1992, p 843-853
- 1999Cha:** D. Chandra and K. Helmy, "X-ray Diffraction and Differential Calorimetry Investigation of Ammonium Nitrate Solid Solutions", Interim Report to TRW Vehicle Safety Systems, 1999